Journal of Southeast University (English Edition) Vol. 29, No. 4, pp. 436 - 440 Dec. 2013 ISSN 1003—7985

Mechanical analysis of transmission lines based on linear sliding cable element

Liu Yun[1,2] Qian Zhendong[2] Xia Kaiquan[3]

([1]College of Civil and Transportation Engineering, Hohai University, Nanjing 210098, China)
([2]Intelligent Transportation System Institute, Southeast University, Nanjing 210096, China)
([3]China Electric Power Research Institute, Beijing 100192, China)

Abstract: In order to study the sliding characteristics when the cable structures are connected with other rods, a string of sliding cable elements (SCE) consisting of one active three-node SCE passing through the sliding point and multiple inactive two-node SCEs is put forward. Based on the updated Lagrangian formulation, the geometric nonlinear stiffness matrix of the three-node straight sliding cable element is deduced. The examples about two-span and three-span continuous cable structures are studied to verify the effectiveness of the derived SCE. Comparing the cable tension of SCE with the existing research results, the calculating results show that the error is less than 1%. The sliding characteristics should be considered in practical engineering because of the obvious difference between the cable tension of the SCE and that of the cable element without considering sliding characteristics.

Key words: transmission line; sliding cable element; updated Lagrangian formulation; geometric nonlinear

doi: 10.3969/j.issn.1003-7985.2013.04.015

High-voltage overhead transmission lines can be idealized as cable-rod-beam coupling systems[1-6]. The cable element is always used to simulate the transmission line, and the truss element is always used to simulate the insulator and the components of the tower. When the transmission lines are connected with other rods, the slippage may occur at a clamp or a joint. Therefore, a new cable element should be developed to consider the influence of the sliding characteristics on the mechanical response of transmission lines.

Some scholars put forward the analysis method considering sliding characteristics. Tang and Shen[7] presented a new finite element model with five-node curved cable elements using quartic polynomial interpolation. Guo and Cui[8] calculated the cable tension on both two sides of the sliding point by applying different temperature loads representing either heating or cooling to each side of the sliding point. Zhang and Dong[9] presented an algorithm for the analysis of the continuous cable in tension structures based on a two-node catenary cable element. Wei and Liu[10] developed a numerical method by the finite element method (FEM) dealing with the cable-sliding problem in cable structures. Aufaure et al.[11-12] presented the three-node finite element formulation of a length of cable passing through a pulley and clamp respectively, i.e. the expressions of the internal forces and of the stiffness matrix. Nie et al.[13] put forward a nonlinear method for calculating the continuous cables sliding at the middle support. Wei[14] developed an effective numerical method for the cable sliding problem in cable structures, and a two-node catenary cable element was built to model the cables based on the analytical solution of elastic catenary. McDonald et al.[15] developed a pulley element which can model a finite length of cable supported somewhere along its length by a pulley. Zhou et al.[16] used the principle of virtual work and the total Lagrange (TL) formulation to derive the element internal force vector and the tangent stiffness matrix. Chen et al.[17] presented the multi-node sliding cable element for the analysis of cable structures with cables threading through a number of joints and being able to slide inside them.

In the previous studies, the formulation of the catenary element used in the group of sliding cables is too complicated to solve in the finite element analysis, and the total Lagrangian formulation is used to derive the tangent stiffness matrix of the active sliding cable. In this paper, the slippage between cables and joint structures in the transmission lines is considered. The geometric nonlinear stiffness matrix of the three-node straight sliding cable element is deduced based on the updated Lagrangian (UL) formulation. Finally, two examples are given to verify the proposed sliding cable element.

1 Finite Element Formulation of Linear Sliding Cable Element

Fig. 1 shows a string of the sliding cable element

Received 2013-05-25.

Biography: Liu Yun (1981—), male, doctor, lecturer, hhu_liuyun@126.com.

Foundation items: The National Natural Science Foundation of China (No. 51308193), China Postdoctoral Science Foundation (No. 20110491342), Jiangsu Planned Projects for Postdoctoral Research Funds (No. 1101018C), the Science and Technology Project of State Grid Corporation of China (No. SGKJ [2007] 116).

Citation: Liu Yun, Qian Zhendong, Xia Kaiquan. Mechanical analysis of transmission lines based on linear sliding cable element[J]. Journal of Southeast University (English Edition), 2013, 29(4): 436 - 440. [doi: 10.3969/j.issn.1003-7985.2013.04.015]

(SCE) consisting of one active three-node SCE passing through the sliding point and multiple inactive two-node SCEs. A special geometrically nonlinear three-node cable element is developed to model the active sliding cables, as shown in Fig. 2. Standard geometrically nonlinear two-node cable elements are used to model the inactive sliding cables. The primary assumption used in this paper to develop the active sliding cable element is that the strain is uniform along the entire element. This assumption implies that there is no resistance, such as friction, at the sliding point. The cross-sectional area of the cable element does not vary with loading, and there is the axial strain in the cable element with no bending moment.

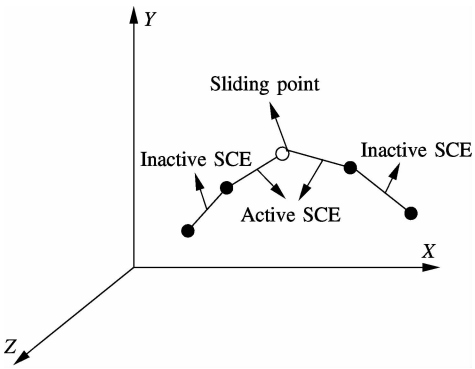

Fig. 1 A group of sliding cables

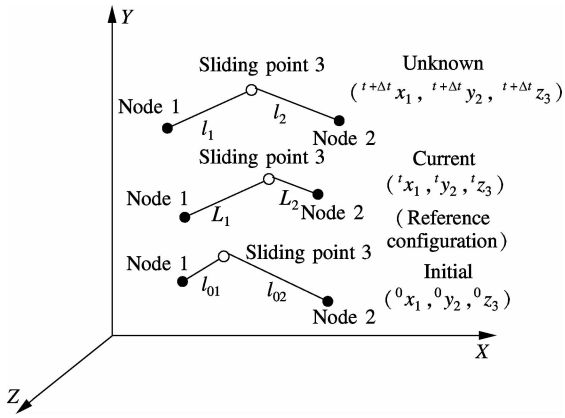

Fig. 2 An active sliding cable element

Fig. 2 shows a definition sketch of an active sliding cable element in its initial, current and unknown configurations. The fundamental kinematic assumption of the sliding cable element states that the strain is uniform along the element; i. e., the strain in both parts is the same at any time. Applying the principle of virtual work and an updated Lagrangian formulation[18], the incremental virtual work done by the internal force is

$$\int_{L_1+L_2}^{t+\Delta t} {}^{t}\boldsymbol{S}_{11}\delta_t^{t+\Delta t}\boldsymbol{\varepsilon}_{11}A_0\mathrm{d}L = {}^{t+\Delta t}W \tag{1}$$

where $\boldsymbol{\varepsilon}_{11}$ is the Green-Lagrange strain; $\boldsymbol{S}_{11}$ is the second Piola-Kirchhoff stress; and A_0 is the initial cross section area of the element, which is assumed to be constant over the entire element length. In the UL formulation, the integration is performed over the current configuration. Because the strain and stress are assumed to be constant along the element, the integration in Eq. (1) is performed analytically as

$${}^{t+\Delta t}W = {}^{t+\Delta t}_{t}\boldsymbol{S}_{11}\delta_t^{t+\Delta t}\boldsymbol{\varepsilon}_{11}A_0(L_1+L_2) \tag{2}$$

where

$${}^{t+\Delta t}_{t}\boldsymbol{S}_{11} = {}^{t}\boldsymbol{\tau}_{11} + {}_{t}\boldsymbol{S}_{11} \tag{3}$$

$${}^{t+\Delta t}_{t}\boldsymbol{\varepsilon}_{11} = {}_{t}\boldsymbol{\varepsilon}_{11} \tag{4}$$

Note that ${}^{t+\Delta t}_{t}\boldsymbol{S}_{11}$ is the second Piola-Kirchhoff stress performed over the current configuration; ${}^{t}\boldsymbol{\tau}_{11}$ is the Cauchy stress tensor performed over the current configuration. ${}_{t}\boldsymbol{S}$ and ${}_{t}\boldsymbol{\varepsilon}$ are, respectively, the Kirchhoff stress increment and the Green strain increment performed over the current configuration.

${}^{0}\boldsymbol{G}_{11}^2$, ${}^{t}\boldsymbol{G}_{11}^2$ and ${}^{t+\Delta t}\boldsymbol{G}_{11}^2$ are the initial, current and unknown components of the metric tensor, respectively[19].

$${}^{0}\boldsymbol{G}_{11}^2 = (L_{01}+L_{02})^2$$
$${}^{t}\boldsymbol{G}_{11}^2 = (L_1+L_2)^2$$
$${}^{t+\Delta t}\boldsymbol{G}_{11}^2 = (l_1+l_2)^2$$

For the three-node sliding cable element, the Green-Lagrange strain is given by

$${}_{0}\boldsymbol{\varepsilon}_{11} = \frac{{}^{t}\boldsymbol{G}_{11}^2 - {}^{0}\boldsymbol{G}_{11}^2}{2} = \frac{(L_1+L_2)^2 - (L_{01}+L_{02})^2}{2} \tag{5}$$

$${}_{t}\boldsymbol{\varepsilon}_{11} = \frac{{}^{t+\Delta t}\boldsymbol{G}_{11}^2 - {}^{t}\boldsymbol{G}_{11}^2}{2} = \frac{(l_1+l_2)^2 - (L_1+L_2)^2}{2} \tag{6}$$

Considering the linearization of the balance equation, ${}_{t}\boldsymbol{S}_{11}$ can be expressed as

$${}_{t}\boldsymbol{S}_{11} = \boldsymbol{D}_{1111\,t}\boldsymbol{\varepsilon}_{11} \tag{7}$$

The second Piola-Kirchhoff stress and the Cauchy stress are given by

$${}_{t}\boldsymbol{S}_{11} = \frac{\boldsymbol{C}_{1111\,t}\boldsymbol{\varepsilon}_{11}}{{}^{t}\boldsymbol{G}_{11}^2} = \frac{E_{t}\boldsymbol{\varepsilon}_{11}}{(L_1+L_2)^4} \tag{8}$$

and

$${}^{t}\boldsymbol{\tau}_{11} = \frac{\boldsymbol{C}_{1111\,0}^{\ t}\boldsymbol{\varepsilon}_{11}}{{}^{0}\boldsymbol{G}_{11}^2} = \frac{E_{0}^{t}\boldsymbol{\varepsilon}_{11}}{(L_{01}+L_{02})^4} \tag{9}$$

where E is Young's modulus. Performing the variation of Eq. (3) yields

$$\delta_{t}\boldsymbol{\varepsilon}_{11} = (l_1+l_2)(\delta l_1+\delta l_2) \tag{10}$$

The initial, current and unknown element length are determined from the respective nodal coordinates (x_i, y_i, z_i) as

$$l_i^2 = ({}^{t+\Delta t}x_3 - {}^{t+\Delta t}x_i)^2 + ({}^{t+\Delta t}y_3 - {}^{t+\Delta t}y_i)^2 + ({}^{t+\Delta t}z_3 - {}^{t+\Delta t}z_i)^2 \qquad i=1,2 \tag{11}$$

$$L_i^2 = ({}^t x_3 - {}^t x_i)^2 + ({}^t y_3 - {}^t y_i)^2 + ({}^t z_3 - {}^t z_i)^2 \qquad i = 1, 2 \tag{12}$$

$$L_{0i}^2 = ({}^0 x_3 - {}^0 x_i)^2 + ({}^0 y_3 - {}^0 y_i)^2 + ({}^0 z_3 - {}^0 z_i)^2 \qquad i = 1, 2 \tag{13}$$

The current nodal coordinates are related to the initial coordinates $({}^0 x_i, {}^0 y_i, {}^0 z_i)$ and the current nodal displacements $({}^t u, {}^t v, {}^t w)$ by

$${}^t x_i = {}^0 x_i + {}^t u_i,\ {}^t y_i = {}^0 y_i + {}^t v_i,\ {}^t z_i = {}^0 z_i + {}^t w_i \qquad i = 1, 2, 3 \tag{14}$$

The unknown nodal coordinates are related to the current coordinates $({}^t x_i, {}^t y_i, {}^t z_i)$ and the current nodal displacements $({}^{t+\Delta t} u, {}^{t+\Delta t} v, {}^{t+\Delta t} w)$ by

$$\begin{aligned} &{}^{t+\Delta t} x_i = {}^t x_i + {}^{t+\Delta t} u_i,\quad {}^{t+\Delta t} y_i = {}^t y_i + {}^{t+\Delta t} v_i \\ &{}^{t+\Delta t} z_i = {}^t z_i + {}^{t+\Delta t} w_i \qquad i = 1, 2, 3 \end{aligned} \tag{15}$$

$$\boldsymbol{\Delta} = \left\{ \frac{\Delta x_1}{l_1} \quad \frac{\Delta y_1}{l_1} \quad \frac{\Delta z_1}{l_1} \quad \frac{\Delta x_2}{l_2} \quad \frac{\Delta y_2}{l_2} \quad \frac{\Delta z_2}{l_2} \quad -\frac{\Delta x_1}{l_1} - \frac{\Delta x_2}{l_2} \quad -\frac{\Delta y_1}{l_1} - \frac{\Delta y_2}{l_2} \quad -\frac{\Delta z_1}{l_1} - \frac{\Delta z_2}{l_2} \right\}^{\mathrm{T}}$$

$$\delta \boldsymbol{d} = \left\{ \delta\, {}^{t+\Delta t} u_1 \quad \delta\, {}^{t+\Delta t} v_1 \quad \delta\, {}^{t+\Delta t} w_1 \quad \delta\, {}^{t+\Delta t} u_2 \quad \delta\, {}^{t+\Delta t} v_2 \quad \delta\, {}^{t+\Delta t} w_2 \quad \delta\, {}^{t+\Delta t} u_3 \quad \delta\, {}^{t+\Delta t} v_3 \quad \delta\, {}^{t+\Delta t} w_3 \right\}^{\mathrm{T}}$$

The incremental virtual work given by Eq. (2) can be rewritten as

$$\delta W_{\mathrm{I}} = \boldsymbol{F}_{\mathrm{I}}^{\mathrm{T}} \delta \boldsymbol{d} = -(\beta_1 + \beta_0)\, \boldsymbol{\Phi} \boldsymbol{\Delta}^{\mathrm{T}} \delta \boldsymbol{d} \tag{19}$$

and the internal force vector is

$$\boldsymbol{F}_I = -(\beta_1 + \beta_0)\, \boldsymbol{\Phi} \boldsymbol{\Delta} \tag{20}$$

where

$$\beta_1 = \frac{E_t \varepsilon_{11} A_0}{(L_1 + L_2)^3},\quad \beta_0 = \frac{E_0' \varepsilon_{11} (L_1 + L_2)}{(L_{01} + L_{02})^4},\quad \boldsymbol{\Phi} = l_1 + l_2$$

Note that the β term is constant. Taking the partial derivative of the internal force with respect to the nodal displacement yields the following element tangent stiffness matrix:

$$\boldsymbol{K}_{\mathrm{t}} = \frac{\partial \boldsymbol{F}_{\mathrm{I}}}{\partial \boldsymbol{d}} = \frac{\partial [-(\beta_1 + \beta_0)\, \boldsymbol{\Phi} \boldsymbol{\Delta}]}{\partial \boldsymbol{d}} = \frac{\partial (-\beta_1 \boldsymbol{\Phi} \boldsymbol{\Delta})}{\partial \boldsymbol{d}} + \frac{\partial (-\beta_0 \boldsymbol{\Phi} \boldsymbol{\Delta})}{\partial \boldsymbol{d}} \tag{21}$$

where

$$\frac{\partial (-\beta_1 \boldsymbol{\Phi} \boldsymbol{\Delta})}{\partial \boldsymbol{d}} = -\frac{EA_0}{(L_1 + L_2)^3} \left(\boldsymbol{\Delta} \frac{\partial\, {}_t \varepsilon_{11} \boldsymbol{\Phi}}{\partial \boldsymbol{d}} + {}_t \varepsilon_{11} \boldsymbol{\Phi} \frac{\partial \boldsymbol{\Delta}}{\partial \boldsymbol{d}} \right) \tag{22}$$

$$\frac{\partial (-\beta_0 \boldsymbol{\Phi} \boldsymbol{\Delta})}{\partial \boldsymbol{d}} = -\beta_0 \left(\boldsymbol{\Delta} \frac{\partial \boldsymbol{\Phi}}{\partial \boldsymbol{d}} + \boldsymbol{\Phi} \frac{\partial \boldsymbol{\Delta}}{\partial \boldsymbol{d}} \right) \tag{23}$$

and

$$\frac{\partial\, {}_t \varepsilon_{11} \boldsymbol{\Phi}}{\partial \boldsymbol{d}} = -[\, {}_t \varepsilon_{11} + (l_1 + l_2)^2]\, \boldsymbol{\Delta}^{\mathrm{T}} \tag{24}$$

Substituting Eq. (15) into Eq. (11) and performing the variation, we can obtain

$$\delta l_i = \frac{1}{l_i} [\, \Delta x_i (\delta^{t+\Delta t} u_3 - \delta^{t+\Delta t} u_i) + \Delta y_i (\delta^{t+\Delta t} v_3 - \delta^{t+\Delta t} v_i) + \Delta z_i (\delta^{t+\Delta t} w_3 - \delta^{t+\Delta t} w_i)\,] \qquad i = 1, 2 \tag{16}$$

where

$$\begin{aligned} &\Delta x_i = {}^{t+\Delta t} x_3 - {}^{t+\Delta t} x_i,\ \ \Delta y_i = {}^{t+\Delta t} y_3 - {}^{t+\Delta t} y_i \\ &\Delta z_i = {}^{t+\Delta t} z_3 - {}^{t+\Delta t} z_i \qquad i = 1, 2 \end{aligned} \tag{17}$$

Substituting Eq. (16) into Eq. (10), the virtual strain term can be written as

$$\delta_t \boldsymbol{\varepsilon}_{11} = -(l_1 + l_2)\, \boldsymbol{\Delta}^{\mathrm{T}} \delta \mathrm{d} \tag{18}$$

where

$$\frac{\partial \boldsymbol{\Delta}}{\partial \boldsymbol{d}} = \begin{bmatrix} \boldsymbol{\theta}_1 & \boldsymbol{0} & -\boldsymbol{\theta}_1 \\ & \boldsymbol{\theta}_2 & -\boldsymbol{\theta}_2 \\ & & \boldsymbol{\theta}_1 + \boldsymbol{\theta}_2 \end{bmatrix}_{9 \times 9} \tag{25}$$

$$\frac{\partial \boldsymbol{\Phi}}{\partial \boldsymbol{d}} = -\boldsymbol{\Delta}^{\mathrm{T}} \tag{26}$$

and

$$\boldsymbol{\theta}_i = \frac{1}{l_i^3} \begin{bmatrix} \Delta x_i^2 - l_i^2 & \Delta x_i \Delta y_i & \Delta x_i \Delta z_i \\ & \Delta y_i^2 - l_i^2 & \Delta y_i \Delta z_i \\ & & \Delta z_i^2 - l_i^2 \end{bmatrix}_{3 \times 3} \qquad i = 1, 2 \tag{27}$$

It should be noted that the element equations, as written, are singular when the slider node coincides exactly with either of the end nodes ($l_i = 0$). The element equations for these limit cases can be derived analytically.

2 Verification Problems

A two-span continuous cable structure and a three-span continuous cable structure are implemented to verify the sliding cable element deduced above.

2.1 Example 1

The initial configuration, without gravity, is the unstressed straight line OP_1P_2 dotted in Fig. 3. O represents the anchorage of the cable on a dead end. P_1 is the first pulley fixed at the foot of an insulator chain CP_1. P_2 is the second pulley fixed on the other dead end. O, P_1 and P_2 are level. We seek the profile adopted by the cable OP_1P_2 when its unstretched length is given. The calculation parameters of this example are defined as follows:

$OP_1 = 8$ m; $P_1P_2 = 12$ m; $q_0 = 0.2$ kN/m; $E = 1.7 \times 10^5$ MPa; $A_0 = 6.74 \times 10^{-5}$ m^2. (E is the modulus of elasticity; A_0 is the cross sectional area; q_0 is the cable weight per unit length.)

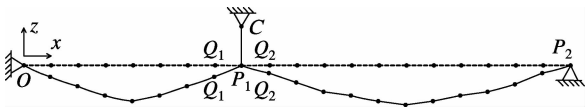

Fig. 3 Equilibrium of a two-span cable with a given unstretched length

Tab. 1 lists the tension of the two kinds of cable structures simulated by the linear space cable element without considering sliding and the linear space cable element considering sliding. As for the linear space cable element, the elastic modulus is modified and an initial strain is applied so that the geometrical non-linearity of the structure should be considered. The tension of the cable structure simulated by the linear space cable element considering sliding is observed to correlate well with the results in Ref. [13]. As shown in Tab. 2, the differences are all within 1%, which indicates the effectiveness and validity of the model adopted in this study. The tension of the cable structure OP_1 simulated by the linear space cable element considering sliding is greater than that of the simulated by the linear space cable element without considering sliding.

Tab. 1 Cable tension of example 1 kN

Cable element	Span	Horizontal tension	Left tension	Right tension
Linear space cable element without considering sliding	OP_1	5.911 3	5.974 2	5.976 3
	P_1P_2	9.731 5	9.804 3	9.805 2
Linear space cable element considering sliding	OP_1	8.261 3	8.294 5	8.306 3
	P_1P_2	8.201 6	8.287 3	8.289 6

Tab. 2 Cable tension in Ref. [13] kN

Cable element	Span	Horizontal tension	Left tension	Right tension
Cable element without considering sliding	OP_1	5.941 3	5.995 2	5.995 3
	P_1P_2	9.751 5	9.825 3	9.825 5
Cable element considering sliding	OP_1	8.310 2	8.348 7	8.348 8
	P_1P_2	8.261 6	8.348 8	8.349 0

2.2 Example 2

A three-span continuous cable structure with non-uniform height supports is applied to verify the element, as shown in Fig. 4. The calculation parameters of this example are defined as follows: $q_0 = 0.2$ kN/m; $E = 1.7 \times 10^5$ MPa; $A_0 = 6.74 \times 10^{-5}$ m^2. The unstressed lengths of each span are 8.26, 12.52, and 16.64 m, respectively. Nodes 2 and 3 are defined as sliding nodes. The tension of the linear sliding cable element is very close to that in Ref. [13] as shown in Tab. 3, which further proves the correctness of the proposed element in this paper.

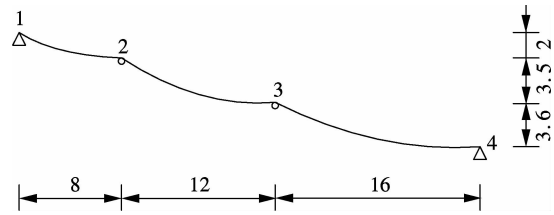

Fig. 4 A three-span unequal height support continuous cable (unit: m)

Tab. 3 Cable tension of example 2

Cable element	Span	Horizontal tension/kN	Left tension/kN	Right tension/kN
Cable element considering sliding in Ref. [13]	12	7.017 5	7.479 4	7.079 6
	23	6.350 0	7.079 6	6.379 8
	34	5.649 0	6.379 8	5.660 3
Linear space cable element considering sliding	12	7.014 55	7.478 66	7.098 77
	23	6.364 34	7.168 55	6.236 77
	34	5.689 92	6.368 55	5.567 76

3 Conclusions

1) The three-node linear sliding cable element is put forward in this paper to consider the slippage in the transmission line structures.

2) The deduced linear sliding cable element is correct and can be used in the analysis of the practical transmission lines structures without considering additional effects, such as friction.

3) Because there is a large difference between the tension of the sliding cable element and that of the cable element without considering sliding, the sliding characteristics should be considered in practical engineering.

References

[1] Roshan F M, McClure G. Numerical modeling of the dynamic response of ice-shedding on electrical transmission lines [J]. *Atmospheric Research*, 1998, **46**(1/2): 1 – 11.

[2] McClure G, Lapointe M. Modeling the structural dynamic response of overhead transmission lines [J]. *Computers and Structures*, 2003, **81**(8/9/10/11): 825 – 834.

[3] Shehata A Y, El Damatty A A, Savory E. Finite element modeling of transmission line under downburst wind loading [J]. *Finite Elements in Analysis and Design*, 2005, **42**(1): 71 – 89.

[4] Hamada A, EI Damatty A A. Behaviour of guyed transmission line structures under tornado wind loading [J]. *Computers and Structures*, 2011, **89**(11/12): 986 – 1003.

[5] Fei Q G, Zhou H G, Han X L, et al. Structural health monitoring oriented stability and dynamic analysis of a long-span transmission tower-line system [J]. *Engineering Failure Analysis*, 2012, **20**: 80 – 87.

[6] Qin L, Yuan J J, Li W. Random wind-induced response analysis of transmission tower-line system [J]. *Energy Procedia*, 2012, **16**: 1813 – 1821.

[7] Tang Jianmin, Shen Zuyan. A nonlinear analysis method

with sliding cable elements for the cable structures [J]. *Chinese Journal of Computational Mechanics*, 1999, **16**(2): 143 - 149. (in Chinese)

[8] Guo Yanlin, Cui Xiaoqiang. A unified analytical method for gliding cable structures: frozen-heated method [J]. *Engineering Mechanics*, 2003, **20**(4): 156 - 159. (in Chinese)

[9] Zhang Zhihong, Dong Shilin. Slipping analysis of continuous cable in tension structures [J]. *Spatial Structures*, 2001, **7**(3): 26 - 32. (in Chinese)

[10] Wei Jiandong, Liu Zhongyu. One method dealing with cable sliding [J]. *Chinese Journal of Computational Mechanics*, 2003, **20**(4): 495 - 499. (in Chinese)

[11] Aufaure M. A finite element of cable passing through a pulley [J]. *Computers and Structures*, 1993, **46**(5): 807 - 812.

[12] Aufaure M. A three-node cable element ensuring the continuity of the horizontal tension: a clamp-cable element [J]. *Computers and Structures*, 2000, **74**(2): 243 - 251.

[13] Nie Jianguo, Chen Bilei, Xiao Jianchun. Nonlinear static analysis of continuous cables with sliding at the middle supportings [J]. *Chinese Journal of Computational Mechanics*, 2003, **20**(3): 320 - 324. (in Chinese)

[14] Wei J D. Cable sliding at supports in cable structures [J]. *Journal of Southwest Jiaotong University*, **12**(1): 56 - 60.

[15] McDonald B M, Peyrot A H. Analysis of cables suspended in sheaves [J]. *Journal of Structural Engineering*, 1988, **114**(3): 693 - 706.

[16] Zhou B, Accorsi M L, Leonard J W. Finite element formulation for modeling sliding cable elements [J]. *Computers and Structures*, 2004, **82**(2/3): 271 - 280.

[17] Chen Z H, Wu Y J, Yin Y, et al. Formulation and application of multi-node sliding cable element for the analysis of Suspen-Dome structures [J]. *Finite Element in Analysis and Design*, 2010, **46**(9): 743 - 750.

[18] Thai H T, Kim S E. Nonlinear static and dynamic analysis of cable structures [J]. *Finite Elements in Analysis and Design*, 2011, **47**(3): 237 - 246.

[19] Green A E, Zerna W. *Theoretical elasticity* [M]. 2nd ed. New York: Dover Publication Inc, 1992: 18 - 22.

基于直线型滑移索单元的输电线路结构张力分析

刘 云[1,2] 钱振东[2] 夏开全[3]

([1] 河海大学土木与交通学院,南京 210098)

([2] 东南大学智能运输系统研究中心,南京 210096)

([3] 中国电力科学研究院,北京 100192)

摘要: 为了研究高压架空输电线索结构与塔架等其他杆件连接处的滑移特性,定义了一组滑移索单元,由一个通过滑动节点连接的三节点活动滑移索单元和多个两节点非活动滑移索单元组成. 基于更新拉格朗日格式推导了三节点直线型滑索单元几何非线性刚度矩阵,并通过两跨和三跨等高连续索结构的有限元数值算例验证了空间直线型滑移索单元的有效性. 研究结果表明,推导的直线型滑移索单元张力与已有计算结果相比,误差在1%以内. 考虑滑移的索结构初始平衡状态内力与不考虑滑移的情况比较相差较大,因而在实际工程中应该考虑索的滑移.

关键词: 输电线路;滑移索单元;更新拉格朗日方程;几何非线性

中图分类号: TM753